

Identification of Rhodium–Rhenium Nonacarbonyl $\text{RhRe}(\text{CO})_9$. Spectroscopic and Thermodynamic Aspects

Chuanzhao Li, Liangfeng Guo, and Marc Garland*

Department of Chemical and Biomolecular Engineering, 4 Engineering Drive 4,
National University of Singapore, Singapore 119260

Received June 3, 2004

The hydrido metal carbonyl $\text{HRe}(\text{CO})_5$ reacts rapidly with the cluster $\text{Rh}_4(\text{CO})_{12}$ at room temperature in *n*-hexane solvent under CO and H_2 to give the coordinately saturated dinuclear carbonyl complex $\text{RhRe}(\text{CO})_9$. At room temperature and low partial pressures of CO and H_2 ($P_1 < 2.2$ MPa), an observable equilibrium is established between the reactants: $4\text{HRe}(\text{CO})_5 + \text{Rh}_4(\text{CO})_{12} + 4\text{CO} \rightarrow 4\text{RhRe}(\text{CO})_9 + 2\text{H}_2$. This observation implies the facile activation of molecular hydrogen on $\text{RhRe}(\text{CO})_9$ at mild conditions and in the presence of CO. A pure component spectrum of $\text{RhRe}(\text{CO})_9$ was obtained by BTEM analysis from the in situ FTIR spectroscopic measurements of the equilibrated solutions. The new species has absorbance maxima at 1985.6(s), 2012.2(w), 2026.6(vs, br), 2075(s), and 2127.2(w) cm^{-1} , indicative of local trigonal bipyramidal geometry on the $-\text{Rh}(\text{CO})_4$ moiety and square bipyramidal geometry on the $-\text{Re}(\text{CO})_5$ moiety. Equilibrium measurements on the temperature interval $T = 289.7\text{--}308.2$ K and the partial pressure intervals 0.2 MPa $< P_{\text{CO}} < 2.2$ MPa and 0.05 MPa $< P_{\text{H}_2} < 2.0$ MPa were performed, providing an enthalpy of reaction $\Delta_r H = -116 \pm 29$ kJ/mol and entropy of reaction $\Delta_r S = -312 \pm 99$ J/(mol K). Attempts to isolate $\text{RhRe}(\text{CO})_9$ by crystallization at -78 °C were unsuccessful.

Introduction

Metal carbonyl compounds have played a rather special historical role in the development of organometallic chemistry since they represent many of the first identified and isolated metal-organics and were used in many of the first detailed metal-organic mechanistic studies.¹ Mononuclear carbonyls of many of the transition metal elements have been synthesized. Additionally, many homometallic dinuclear and polynuclear carbonyl clusters have been synthesized.² Metal carbonyls are frequently used for stoichiometric as well as catalytic metal-mediated organic syntheses, to introduce organo-carbonyl functionalities.³ In turn, carbonyl-containing functional groups are widely considered to be the backbone of many further synthetic strategies.⁴

Considerable interest in simple hetero-bimetallic metal carbonyls exists. Much of this interest arises from (a) outstanding structural questions, (b) the desire to further understand basic reaction mechanisms particularly where activation of small molecules occurs, and (c) the need to explain the observation of synergism in many bimetallic metal-mediated organic syntheses. Although a large variety of bimetallic polynuclear

carbonyls have been synthesized and characterized, the same cannot be said of the most simple mixed-metal organometallics, namely, unsubstituted hetero-bimetallic dinuclear carbonyls. An extensive list of known unsubstituted hetero-bimetallic dinuclear carbonyls is provided in Table 1.

The species listed in Table 1 have a number of interesting attributes, but particular noteworthy are the nonisolatability and reactivity under mild conditions of some of these species. For example, $\text{CoRh}(\text{CO})_7$ is nonisolatable,¹² it readily reacts with molecular hydrogen at subambient temperatures,¹⁴ and it initiates fairly

* To whom correspondence should be addressed. Phone: +65-6-874-6617. Fax: +65-6-779-1936. E-mail: chemvg@nus.edu.sg.

(1) Basolo, F.; Ralph, G. P. *Mechanisms of inorganic reactions; a study of metal complexes in solution*; Wiley: New York, 1958.

(2) (a) Housecroft, C. E. *Metal–metal bonded carbonyl dimers and clusters*; Oxford University Press: New York, 1996. (b) Dyson, P. J.; McIndoe, J. S. *Transition metal carbonyl cluster chemistry*; Gordon and Breach Science Publishers: The Netherlands, 2000.

(3) Wender, I.; Pino, P. *Organic syntheses via metal carbonyl*; Wiley: New York, 1977; Vol. 1 and Vol. 2.

(4) Seebach, D.; Weidmann, B.; Widler, L. In *Modern Synthetic Methods*; Scheffold, R., Ed.; Otto Salle Verlag: Frankfurt, 1983; p 324.

(5) (a) Joshi, K. K.; Pauson, P. L. *Z. Naturforsch.* **1962**, 17b (8), 565. (b) Bor, G.; Sbrignadello, G. *J. Chem. Soc., Dalton Trans.* **1974**, (4), 440–8. (c) Beck, K.; Alexander, J.; Krause Bauer, J. A.; Nauss, J. L. *Inorg. Chim. Acta* **1999**, 288 (2), 159–173.

(6) Addison, S. J.; Connor, J. A.; Kinkaid, J. A. *J. Organomet. Chem.* **1998**, 554 (2), 123–127.

(7) Kovacs, I.; Hoff, C.; Ungvary, F.; Marko, L. *Organometallics* **1985**, 4, 1347–1350.

(8) (a) Kruck, T.; Hoefler, M. *Ber.* **1964**, 97 (8), 2289–300. (b) Kruck, T.; Hoefler, M. *Angew. Chem.* **1964**, 76 (18), 786.

(9) Sbrignadello, G.; Tomat, G.; Magon, L.; Bor, G. *Inorg. Nucl. Chem. Lett.* **1973**, 9 (10), 1073–1077.

(10) (a) Nesmeyanov, A. N.; Anisimov, K. N.; Kolobova, N. E.; Kolomnikov, I. S. *Ser. Khim.* **1963**, 194. (b) Sbrignadello, G.; Batiston, G.; Bor, G. *Inorg. Chim. Acta* **1975**, 14 (1), 69–78. (c) Knox, S. A. R.; Hoxmeier, R. J.; Kaesz, H. D. *Inorg. Chem.* **1971**, 10 (11), 2636–2637. (d) Michels, G. D.; Svec, H. J. *Inorg. Chem.* **1981**, 20 (10), 3445–3447.

(11) Martin, B.; Warner, D. K.; Norton, J. R. *J. Am. Chem. Soc.* **1986**, 108 (1), 33–39.

(12) (a) Spinder, F.; Bor, G.; Dietler, U. K.; Pino, P. *J. Organomet. Chem.* **1981**, 213, 303. (b) Garland, M.; Horvath, I. T.; Bor, G.; Pino, P. *Organometallics* **1986**, 10, 559–567. (c) Horvath, I. T.; Bor, G.; Garland, M.; Pino, P. *Organometallics* **1986**, 5 (7), 1441–1445.

(13) Garland, M.; Horvath, I. T.; Bor, G.; Pino, P. *Organometallics* **1991**, 10, 559–567.

(14) (a) Horvath, I.; Garland, M.; Bor, G.; Pino, P. *J. Organomet. Chem.* **1988**, 358, C17–C22. (b) Garland, M.; Pino, P. *Organometallics* **1990**, 9, 1943–1949.

Table 1. List of Known Unsubstituted Hetero-bimetallic Dinuclear Carbonyls and Relevant References to Their Characterization

species	refs for syntheses and characterization	refs for thermodynamics	refs for mechanistic studies	refs for catalysis
CoMn(CO) ₉	5	6	7	
CoRe(CO) ₉	5b, 8	6		
CoTc(CO) ₉	5b, 9			
ReMn(CO) ₁₀	10	6	11	
MnTc(CO) ₁₀	10b, 10d			
ReTc(CO) ₁₀	10b, 10d			
CoRh(CO) ₇	12	13	14	14b, 15, 18
CoRh(CO) ₈	12b	13	14	14, 15
RhRe(CO) ₉	this work	this work	this work	

rapid catalytic hydroformylation at ambient or even subambient temperatures at a total CO/H₂ pressure of 0.1 MPa.¹⁵ These conditions are similar to those for the Wilkinson catalyst HCoRh(PPh₃)₃.¹⁶ The synergism observed in catalytic hydroformylation with CoRh(CO)₇ as precursor has been attributed to (a) facile hydrogen activation and subsequent generation of HRh(CO)₃/HRh(CO)₄ for the active rhodium cycle at low temperatures¹⁷ and (b) cluster catalysis at high temperatures.¹⁸ As noted previously, low temperature activation of molecular hydrogen is often very difficult to achieve particularly in the presence of carbon monoxide.^{14,19}

Further, in the context of synergism, it can be mentioned that the existence of highly reactive hetero-bimetallic dinuclear carbonyls MnRh(CO)₉/MnRh(CO)₈ has been postulated in recent low-temperature hydroformylations where HMn(CO)₅ and RCoRh(CO)₄ are simultaneously observed under catalytic reaction conditions. A new catalytic reaction topology, called bimetallic catalytic binuclear elimination, has been invoked to explain the kinetics. The active catalytic system consists of three sets of intermediates: mononuclear manganese, mononuclear rhodium, and hetero-bimetallic dinuclear species.²⁰

In the present contribution the synthesis and characterization of the new hetero-bimetallic dinuclear carbonyl RhRe(CO)₉ is presented.

Experimental Section

General Information. All solution preparations and transfers were carried out under purified argon (99.9995%, Saxol, Singapore) atmosphere using standard Schlenk techniques.²¹ The argon was further purified before use by passing it through a deoxy and zeolite column. Purified carbon monoxide (research grade, 99.97%, Saxol, Singapore) and purified hy-

(15) Garland, M. Low-temperature homogeneous catalytic hydroformylation with mixed cobalt and rhodium carbonyls as catalyst precursors, Ph.D. Thesis, ETH No 8585, 1988.

(16) (a) Osborn, J. A.; Jardine, F. H.; Young, J. F.; Wilkinson, G. *J. Am. Chem. Soc.* **1966**, *12*, 1711–1732. (b) Evans, D.; Yagupsky, G.; Wilkinson, G. *J. Am. Chem. Soc.* **1968**, *11*, 2660–2665. (c) Yagupsky, G.; Brown, C. K.; Wilkinson, G. *J. Am. Chem. Soc.* **1970**, *9*, 1392–1401.

(17) Garland, M. *Organometallics* **1993**, *12*, 535–543.

(18) Ojima, I.; Li, Z. Catalysis of Rh, Rh–Co, and Ir–Co multinuclear complexes and its applications to organic syntheses. In *Catalysis by Di- and Polynuclear Metal Cluster Complexes*; Adams, R. D., Cotton, F. A., Eds.; Wiley-VCH: New York, 1998; pp 307–343.

(19) (a) Halpern, J. *Adv. Catal.* **1959**, *11*, 301. (b) Pino, P.; Oldani, F.; Consiglio, G. *J. Organomet. Chem.* **1983**, 250491.

(20) (a) Li, C.; Widjaaj, E.; Garland, M. *J. Am. Chem. Soc.* **2003**, *125* (18), 5540–5548. (b) Li, C.; Widjaaj, E.; Garland, M. *Organometallics* **2004**, *23* (17), 413–418.

(21) Shriver, D. F.; Drezzdon, M. A. *The Manipulation of Air-Sensitive Compounds*; Wiley: New York, 1986.

Table 2. Experimental Design

expt	step	P _{H₂} , MPa	P _{CO} , MPa	Rh ₄ (CO) ₁₂ , mg	HRe(CO) ₅ , μL	hexane, mL	T, K
1	1	0.11	0.31	88.68	58	250	289.7
	2	0.21	0.31	88.68	58	250	289.7
	3	0.31	0.31	88.68	58	250	289.7
	4	0.51	0.31	88.68	58	250	289.7
2	1	0	2.0	77.87	70.0	250	298.3
	2	1.0	2.0	77.87	70.0	250	298.3
	3	2.0	2.0	77.87	70.0	250	298.3
3	1	0.05	0.2	83.86	70.0	250	298.3
	2	0.10	0.2	83.86	70.0	250	298.3
	3	0.15	0.2	83.86	70.0	250	298.3
4	4	0.40	0.2	83.86	70.0	250	298.3
	1	0.05	0.4	168.88	55.0	250	298.3
	2	0.10	0.4	168.88	55.0	250	298.3
	3	0.15	0.4	168.88	55.0	250	298.3
	4	0.20	0.4	168.88	55.0	250	298.3
5	5	0.40	0.4	168.88	55.0	250	298.3
	1	0.11	0.4	160.75	42.0	250	308.2
	2	0.21	0.4	160.75	42.0	250	308.2
	3	0.42	0.4	160.75	42.0	250	308.2
	4	0.80	0.4	160.75	42.0	250	308.2
6	5	0.8	0.8	160.75	42.0	250	308.2
	1	0.0	1.6	124.9	64.5	250	308.2
	2	1.0	1.6	124.9	64.5	250	308.2
	3	1.58	1.6	124.9	64.5	250	308.2
	4	2.0	1.6	124.9	64.5	250	308.2
5	2.0	2.2	124.9	64.5	250	308.2	

drogen (99.9995%, Saxol, Singapore) were also further purified through deoxy and zeolite columns before they were used. Purified nitrogen (99.9995%, Saxol, Singapore) was used to purge the Perkin-Elmer FT-IR spectrometer system.

Rh₄(CO)₁₂ (98%) and Re₂(CO)₁₀ (99%) were purchased from Strem Chemicals (Newport, MA) and was used as obtained. HRe(CO)₅ was custom synthesized by Strem Chemicals.

Apparatus. In situ kinetic studies were performed in a 1.5 L stainless steel (SS316) autoclave (P_{\max} = 22.5 MPa, Buchi-Uster, Switzerland), which is connected with a high-pressure infrared cell. The system is the same as that used previously.²²

In Situ Spectroscopic Studies. An experimental design was planned, which would utilize the semibatch approach and algorithm.²³ All the experiments were performed in a similar manner. For example, first, single-beam background spectra of the IR sample chamber were recorded. Then 150 mL of *n*-hexane was transferred under argon to the autoclave. Under 0.2 MPa CO pressure, infrared spectra of the *n*-hexane in the high-pressure cell were recorded. The total system pressure was raised to the set CO pressure, and the stirrer and high-pressure membrane pump were started. After equilibration, infrared spectra of the CO/*n*-hexane solution in the high-pressure cell were recorded. A solution of Rh₄(CO)₁₂ dissolved in 50 mL of *n*-hexane was prepared, transferred to the high-pressure reservoir under argon, pressured with CO, and then added to the autoclave. After equilibration, infrared spectra of the Rh₄(CO)₁₂/CO/*n*-hexane/solution in the high-pressure cell were recorded. A solution of HRe(CO)₅ dissolved in 50 mL of *n*-hexane was prepared, transferred to the high-pressure reservoir under argon, pressured with CO, and then added to the autoclave. In the following steps, the semibatch experiment methodology was performed, namely, the CO/H₂ pressures were varied in each semibatch step. Once the system reached equilibrium, the CO/H₂ pressures were varied to conduct the next semibatch step. The detailed experimental design is shown in Table 2.

The experimental design of the experiments involved 250 mL of solvent and the intervals 289.7–308.2 K, P_{H_2} = 0–2.0

(22) Feng, J.; Garland, M. *Organometallics* **1999**, *18* (3), 417–427.

(23) Widjaja, E.; Li, C.; Garland, M. *Organometallics* **2002**, *21*, 1991–1997.

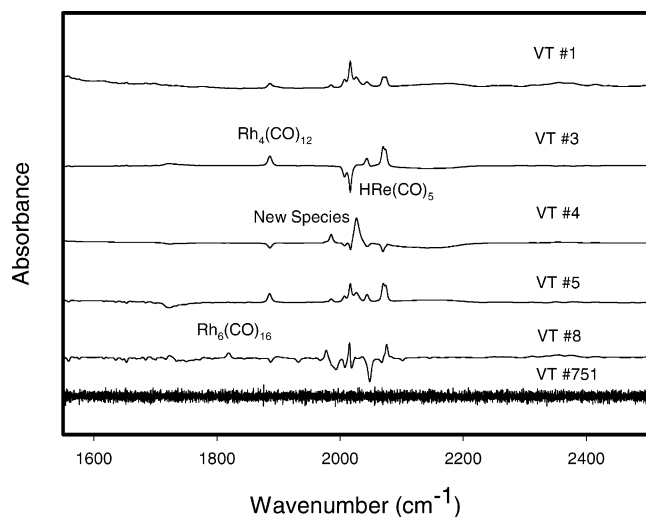


Figure 1. Singular value decomposition of the in situ spectroscopic data showing the first, third, fourth, and fifth significant vectors and the 751th vector. The marked extrema are those that were used to recover the organometallic pure component spectra by BTEM.

MPa, $P_{CO} = 0.2\text{--}2.2$ MPa, initial $Rh_4(CO)_{12} = 77.87\text{--}168.88$ mg, and initial $HRe(CO)_5 = 42.0\text{--}64.5$ μL .

The in situ spectra were taken every 10 min in the range $1000\text{--}2500$ cm^{-1} with a resolution of 4 cm^{-1} . Since equilibrium was normally established in hours, most of these spectra were recorded under nonequilibrium conditions. A total of 751 spectra were obtained for further spectroscopic analyses.

Attempt at Isolation/Crystallization. $HRe(CO)_5$ (40 μL) was reacted with 80.5 mg of $Rh_4(CO)_{12}$ at room temperature in 200 mL of *n*-hexane solvent under 2.0 MPa CO and in the absence of added H_2 for 6 h. The bright orange reaction mixture was then released to a 250 mL Schlenk tube and cooled with dry ice for 24 h under CO protection. Some orange solids were obtained after removing solvent/dissolved CO, and these were analyzed with FTIR. The spectra obtained are distinctly different than the solution spectrum of $RhRe(CO)_9$.

Results and Discussions

Spectral Analyses. BTEM was used to analyze the spectral data and obtain pure component spectra.²⁴ A total of 751 spectra were obtained in the experiments. Singular value decomposition (SVD) was employed first to decompose the experimental absorbance data matrix $A_{751 \times 4751}$, without any preconditioning,²⁵ to give the orthonormal matrixes $U_{751 \times 751}$ and $V_{4751 \times 4751}^T$.

The significant spectral extrema in the first few right singular vectors ($V_{751 \times 4751}^T$) were inspected and were used as targets in the BTEM algorithm. These noteworthy right singular vectors are presented in Figure 1. Four significant bands, as indicated by the numbers in Figure 1, are highlighted. These bands are prominent spectral features associated with the organometallics present and were targeted by BTEM.

(24) (a) Chew, W.; Widjaja, E.; Garland, M. *Organometallics* **2002**, *21*, 1982–1990. (b) Li, C.; Widjaja, E.; Chew, W.; Garland, M. *Angew. Chem. Int. Ed.* **2002**, *20*, 3785–3789. (c) Widjaja, E.; Li, C.; Garland, M. *Proceeding of the International Conference on Scientific & Engineering Computation (IC-SEC)*, Recent Advances in Computational Sciences and Engineering; Lee, H. P., Kumar, K., Eds.; Imperial College Press: London, 2002; pp 36–40. (d) Widjaja, E.; Li, C.; Chew, W.; Garland, M. *Anal. Chem.* **2003**, *75*, 4499–4507. (e) Widjaja, E.; Li, C.; Garland, M. *J. Catal.* **2004**, *223* (2), 278–289.

(25) Chen, Li; Garland, M. *Appl. Spectrosc.* **2002**, *56* (11), 1422–1428.

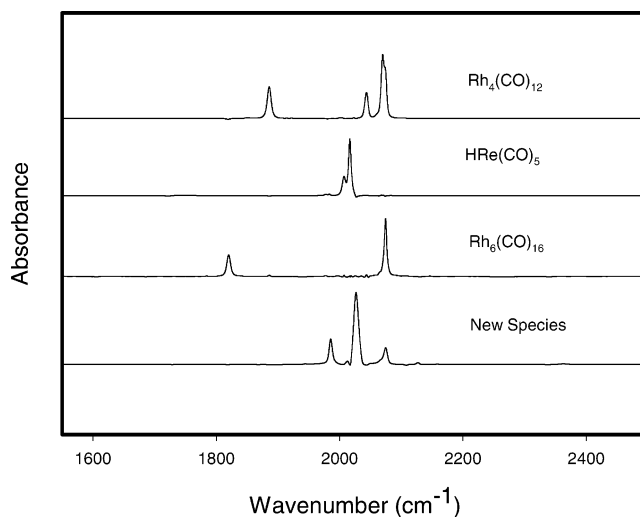


Figure 2. Recovered pure component spectra of the organometallic species using BTEM.

The targeting of the highlighted bands in Figure 1 resulted in four pure component organometallic spectra. The reconstructed pure component spectra via BTEM are presented in Figure 2. These spectra were $Rh_4(CO)_{12}$, $HRe(CO)_5$, $Rh_6(CO)_{16}$, and a new species. The new species has peaks at 1985.6 (s), 2012.2 (w), 2026.6 (vs, br), 2075 (s), and 2127.2 (w) cm^{-1} . Exhaustive use of BTEM on the remaining features in Figure 1 did not result in the recovery of any additional organometallic spectra.

Since the IR spectrum of the new species has no features indicating bridging C–O groups, a higher nuclearity cluster involving two or more Rh atoms is unlikely. Indeed, all known mixed Rh–M clusters having two or more Rh atoms have bridging carbonyls. Good examples include $Co_2Rh_2(CO)_{12}$, $CoRh_3(CO)_{12}$, $Rh_2\text{-}Ir_2(CO)_{12}$, and $Rh_3Ir(CO)_{12}$.^{14,26} Consequently, a low-nuclearity mixed rhodium and rhenium carbonyl is suspected. The simplest example would be a dinuclear complex with a single metal–metal bond and coordinatively saturated moieties $-\text{Rh}(\text{CO})_4$ and $-\text{Re}(\text{CO})_5$.

It is known that the local symmetry of the $-\text{Rh}(\text{CO})_4$ group is C_{3v} and the local symmetry of the $\text{Re}(\text{CO})_5$ group is C_{4v} .²⁷ Figure 3 presents the IR spectra of $\text{BrRe}(\text{CO})_5$ and $\text{HRh}(\text{CO})_4$ ^{16b,28} obtained in our lab for comparison with the new species. As shown in Figure 3, $\text{BrRe}(\text{CO})_5$ has three vibrations at 1986 (s), 2016.4 (w), and 2046 (vs) cm^{-1} and $\text{HRh}(\text{CO})_4$ has three metal–carbonyl vibrations at 2041.6 (vs), 2071.8 (m), and 2123.6 (w) cm^{-1} . Assuming that the two “local symmetries”²⁹ rule holds for a species $(\text{CO})_4\text{Rh}-\text{Re}(\text{CO})_5$, we would expect six bands, three ($2A_1+1E$) for the $\text{Rh}(\text{CO})_4$ part of the molecule and another three ($2A_1+1E$) for the $\text{Re}(\text{CO})_5$ part of the molecule. Accordingly, two very strong bands (E) should be found in the spectrum. The intensity ratio of the two very strong bands (E) should be ca.

(26) Martinengo, S.; Chini, P.; Albano, V. G.; Gariati, F. *J. Organomet. Chem.* **1973**, *59*, 379–394.

(27) Braterman, P. S. *Metal Carbonyl Spectra*; Academic Press: New York, 1973; pp 155–177.

(28) (a) Whyman, R. In *In situ spectroscopic studies in homogeneous catalysis*; Advances in Chemistry Series 230; 1992; pp 19–31. (b) Vidal, J. L.; Walker, W. E. *Inorg. Chem.* **1981**, *20*, 249–54.

(29) Cotton, F.; Liehr, A. D.; Wilkinson, G. *J. Inorg. Nucl. Chem.* **1956**, *2*, 141–148.

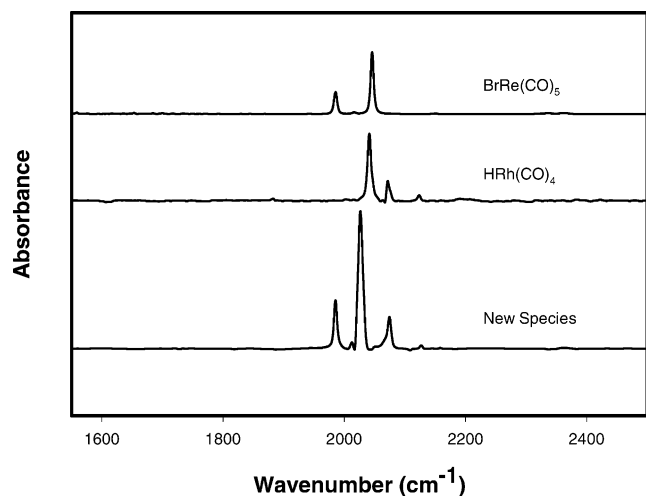
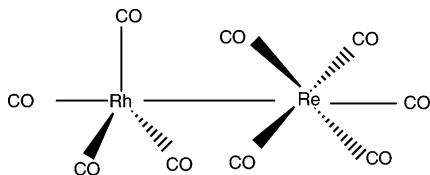


Figure 3. Spectral comparison of the new species with the spectra of $\text{BrRe}(\text{CO})_5$ and $\text{HRh}(\text{CO})_4$ obtained in our lab.

Scheme 1. Proposed Structure of $\text{RhRe}(\text{CO})_9$



3/4, and they should represent ca. 7/9 of the total CO stretching intensities.

Indeed, the new spectrum appears to meet the above assumptions. The two bands $2075(\text{s})$ and $2127.2(\text{w}) \text{ cm}^{-1}$ are quite close to the $2A_1$ belonging to the $\text{Rh}(\text{CO})_4$ moiety, while the other two bands $1985.6(\text{s})$ and $2012.2(\text{w}) \text{ cm}^{-1}$ are quite close to $2A_1$ belonging to the $\text{Re}(\text{CO})_5$ moiety. Furthermore, close inspection of the spectrum indicates that the peak at 2026.6 cm^{-1} is very strong and broad (the half-width is ca. 10 cm^{-1} instead of the usual 5 cm^{-1} anticipated) and is accordingly a combination of the two required strong bands (E). Integrated intensities at this position account for ca. 74% of the total CO stretching intensities.

As mentioned in regard to Table 1, the cobalt–rhenium nonacarbonyl is known. Bor et al.⁵ reported that $\text{ReCo}(\text{CO})_9$ has six peaks at $1971.7(\text{w}, \text{br})$, $1990(\text{s})$, $2007(\text{w})$, $2032.8(\text{vs})$, $2059.8(\text{s})$, and $2133.9(\text{w}) \text{ cm}^{-1}$. Except for the weak broad peak at 1971.7 cm^{-1} , all the other peaks are quite similar to the present new complex. In their assignment, a “free rotational model” was employed to explain the peak at 1971.7 cm^{-1} . Bor et al. also reported that the presence of the isotopic satellite (1956 cm^{-1}) from natural ^{13}C . An ^{13}C isotopic satellite for the lowest vibration at 1944.8 cm^{-1} can be found in the new complex $\text{RhRe}(\text{CO})_9$. The proposed structure for $\text{RhRe}(\text{CO})_9$ is shown in Scheme 1. The attempts to isolate $\text{RhRe}(\text{CO})_9$ by crystallization were unsuccessful. (See Experimental Section for more details.)

Concentration Profiles. Figure 4 shows the time-dependent moles of $\text{Rh}_4(\text{CO})_{12}$, $\text{HRe}(\text{CO})_5$, and $\text{RhRe}(\text{CO})_9$ respectively for experiment 6 (Table 2). As all the peaks of the $\text{HRe}(\text{CO})_5$ are overlapping with other species, its calculation is somewhat sensitive.

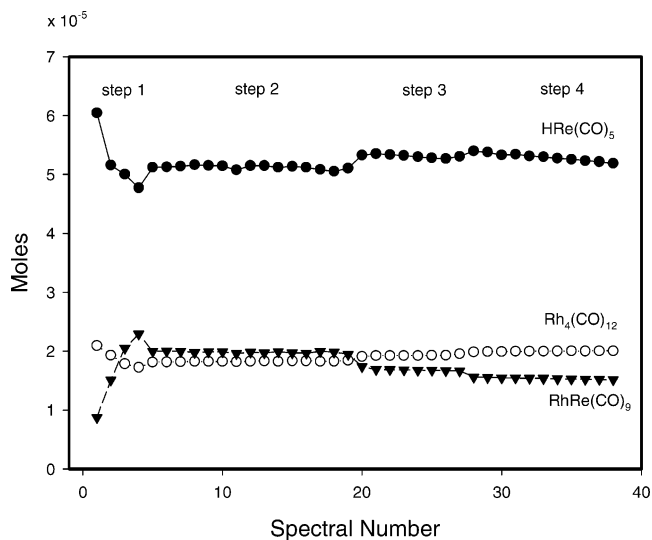
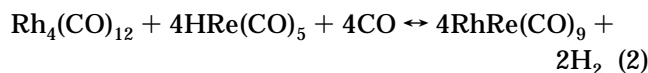


Figure 4. Representative example of the concentration profiles of the organometallic species. This experiment was performed with 250 mL of *n*-hexane at 308.2 K with 0–2.2 MPa CO and 0–2.0 MPa H_2 . The initial conditions were 124.9 mg of $\text{Rh}_4(\text{CO})_{12}$ and 64.5 μL of $\text{HRe}(\text{CO})_5$.

As shown in Figure 4, step 1, with only $\text{Rh}_4(\text{CO})_{12}/\text{HRe}(\text{CO})_5/\text{CO}$ in the system, the moles of both $\text{Rh}_4(\text{CO})_{12}$ and $\text{HRe}(\text{CO})_5$ have a very rapid decline, while the moles of $\text{RhRe}(\text{CO})_9$ increased rapidly. This means that with little or no molecular hydrogen in the system, the reaction $\text{Rh}_4(\text{CO})_{12} + 4\text{HRe}(\text{CO})_5 + 4\text{CO} \leftrightarrow 4\text{RhRe}(\text{CO})_9 + 2\text{H}_2$ goes very fast to the right-hand side. In step 2, when molecular hydrogen was added, it can be seen that the $\text{RhRe}(\text{CO})_9$ moles decreased, and accordingly the moles of both $\text{Rh}_4(\text{CO})_{12}$ and $\text{HRe}(\text{CO})_5$ increased until they reached a new equilibrium state. This is clear evidence for the rapid and reversible molecular hydrogen activation by the heterometallic dinuclear carbonyl $\text{RhRe}(\text{CO})_9$. In the following steps, with more hydrogen introduced in the reactor, similar trends can be observed in Figure 4.

Thermodynamics. Six series of experiments were conducted at three temperatures to determine the equilibrium constants for the reaction.



$$K_{\text{eq}} = \frac{[\text{RhRe}(\text{CO})_9]^4 [\text{H}_2]^2}{[\text{Rh}_4(\text{CO})_{12}] [\text{HRe}(\text{CO})_5]^4 [\text{CO}]^4} \quad (3)$$

In the above equations, all the concentrations were measured in mole fractions. As shown in Table 2, the equilibrium experiments were performed under different partial pressures of CO and H_2 with different initial loadings of $\text{Rh}_4(\text{CO})_{12}$ and $\text{HRe}(\text{CO})_5$.

The regression analyses yield the equilibrium constants at different temperatures. The equilibrium constants were $K_{\text{eq}}(289.7 \text{ K}) = 94\,113$ ($R^2 = 0.88$), $K_{\text{eq}}(298.3 \text{ K}) = 16\,715$ ($R^2 = 0.99$), and $K_{\text{eq}}(308.2 \text{ K}) = 3278$ ($R^2 = 0.89$). The R^2 values indicate that two of the three regressions could be better. The difficulties responsible for the two low R^2 values include (1) the known difficulties in measuring the equilibria of very reactive organometallics,¹³ i.e., $\text{CoRh}(\text{CO})_7$, (2) the deviation in

the CO and H₂ Henry constants in the binary gas vapor–liquid equilibria, and (3) the extremely large values of the exponents in both the numerator and denominator of the equilibrium constant. The latter sixth- and ninth-order dependencies are most surely a significant source of error. Nevertheless, the equilibrium data are consistent with the overall reaction stoichiometry.

The equilibrium thermodynamics was regressed to provide the thermodynamic parameters $\Delta_r H = -116 \pm 29$ kJ/mol and $\Delta_r S = -312 \pm 99$ J/(mol K). The negative value of the enthalpy $\Delta_r H$ is consistent with the observation of higher conversion to the hetero-bimetallic dinuclear complex RhRe(CO)₉ at lower temperatures. In addition, the negative sign of the entropy of the reaction $\Delta_r S$ is in agreement with the stoichiometric equation for this reaction; namely, nine molecule reagents give only six molecules as products. Due to the very low experimental ΔP_T used in this study, a three-parameter thermodynamic expression involving $\Delta_r V$ was not used to analyze the data.

Discussion

It was somewhat surprising not to find Re₂(CO)₁₀ in the reaction of HRe(CO)₅/Rh₄(CO)₁₂ under CO/H₂. Indeed, the HRe(CO)₅ might be expected to undergo bimolecular elimination to form Re₂(CO)₁₀, but this reaction is apparently negligible under the present conditions.

The formation of RhRe(CO)₉ was also attempted without the use of HRe(CO)₅. One semibatch experiment was performed with a reactant combination comprising Re₂(CO)₁₀ and Rh₄(CO)₁₂ in *n*-hexane under 2.0–3.0 MPa CO and 2.0 MPa H₂, at 298–308 K. Spectral analysis with both BTEM and target factor analysis (TFA)^{24e} did not provide any evidence for the presence of ReRh(CO)₉.

The intrinsic reaction kinetics for the formation of RhRe(CO)₉ and/or the activation of molecular hydrogen on RhRe(CO)₉ were too rapid to be captured with the present experimental setup. Indeed, characteristic times for gas–liquid mass transfer as well as liquid-phase mixing were on the order of a few minutes.³⁰ Therefore, it is quite possible, indeed probable, that transport-controlled rather than intrinsic kinetics was observed. Nevertheless, it appears likely that an intermediate such as an unobservable H₂RhRe(CO)₈ and/or H₂RhRe(CO)₇ is formed and subsequently undergoes fragmenta-

tion to give HRe(CO)₅ and a very unstable hydridorhodium species such as HRh(CO)₄^{24b,28} and/or HRh(CO)₃,³¹ rapidly yielding Rh₄(CO)₁₂.

The relatively infrequent identification of a new unsubstituted hetero-bimetallic dinuclear carbonyl probably justifies a small discussion of potential reactivity patterns. Foremost among these reactivity patterns would be the chemistry of the carbonyl ligands. The rapid hydrogen activation on the coordinately saturated RhRe(CO)₉ is a certain indication of facile CO dissociation. In this regard, the rapid dissociation of CO and subsequent hydrogen activation is similar to the case of CoRh(CO)₈: both occur at room temperature under significant partial pressures of CO. Furthermore, the issue of facile CO dissociation prompts questions about fluxionality. It is well known that the CO ligands on Rh₄(CO)₁₂,³² but more importantly CoRh(CO)₇/CoRh(CO)₈, are fluxional on the NMR time scale. This issue is surely one that should be addressed in the future.

The CO dissociation also prompts questions about possible facile substitution reactions. Substitution with 1 equiv of phosphine almost surely occurs, and substitution on the rhodium is the probable position, as is the case for CoRh(CO)₇ + PEt₃ → CoRh(CO)₆PEt₃ + CO.³³ Analogously, substitutions with NR₃, PPN, etc., can be expected. More complex addition reactions involving unsaturated organic molecules should not be ruled out either. It is known that CoRh(CO)₇ readily adds 1 equiv of alkyne (C₆F₅C≡CC₆F₅, PhC≡CPh) to make CoRh(CO)₆(μ-η²-alkyne).³⁴ A related reaction with RhRe(CO)₉ may occur.

The known facile CO dissociation and rapid activation of molecular hydrogen and the presumed reactivity toward addition reactions suggest the strong potential for RhRe(CO)₉ as a catalyst precursor in a variety of catalytic syntheses, but particularly carbonylations. Future work in this area is planned.

Acknowledgment. Financial support for this experimental research was provided by the Academic Research Fund of the National University of Singapore (NUS). Research scholarships for C.L. and L.G. were provided by the Graduate School of Engineering (NUS). C.L. also thanks Singapore Millenium Foundation (SMF) for a SMF postdoctoral fellowship.

OM0496030

(31) Chini, P.; Martinengo, S. *Inorg. Chim. Acta* **1969**, 3, 21.

(32) Evans, J.; Johnson, B. F. G.; Lewis, J.; Norton, J.R.; Cotton, F. A. *J. Chem. Soc., Chem. Commun.* **1973**, 807.

(33) Horvath, I. T. *Organometallics* **1986**, 5 (11), 2333–2340.

(34) (a) Horvath, I. T.; Zsolnai, L.; Huttner, G. *Organometallics* **1986**, 5 (1), 180–182. (b) Horvath, I. T. *Polyhedron* **1988**, 7 (22–23), 2345–2349.

(30) Garland, M. Transport Effects in Homogeneous Catalysis. In *Encyclopedia of Catalysis*; Horvath, I. T., Ed.; Wiley: New York, 2002.